in our earlier work [14], there is reason to believe that the algorithm can be used with any mobile manipulator system.

A potential problem associated with using simulated annealing is that it may require an excessive amount of computer time. The data for Figs. 3, 5, and 6 were obtained on a Micro Vax II. We required an average of only 45 s of CPU time to solve the two-task problem, while the four-task problem required 140 to 170 s to solve depending on whether a cyclic solution was desired or not. These solution times are of the same order of magnitude as those achieved in [14] and were achieved without optimizing our simulated annealing algorithm for speed.

## VI. Summary

In this work we have formulated a sequential task problem for a mobile manipulator as a global optimization problem. The mobile manipulator system redundancies allow a number of tasks to be performed for some minimum cost. The tasks are defined simply by desired positions and orientations and desired forces and moments, and the cost is defined by the length of the trajectory of the mobile base. This cost is representative of a measure of time or energy required to position and orient the system for each task. We note that these definitions produce a nonlinear cost function with nonlinear and nonconvex constraints and unconnected regions, and demonstrate that satisfactory solutions can be obtained through the use of simulated annealing. While the computational time required for this optimization increases with the complexity of the system and the number of tasks to be performed, it is not excessive, and the optimization, performed offline, could result in tremendous savings if a series of tasks is to be repeated many times.

## References


[1] R. Mann, W. Hamel, and C. Weisbin, "The development of an intelligent nuclear maintenance robot," in *Proc. IEEE Int. Conf. Robotics Automat.*, 1988.

[2] R. Carlton and S. Bartholet, "The evolution of the application of mobile robotics to nuclear facility operations and maintenance," in *Proc. IEEE Int. Conf. Robotics Automat.*, 1987, pp. 720-726.

[3] T. Yoshikawa, "Analysis and control of robot manipulators with redundancy," in *Robotics Research: The First Int. Symp.* Cambridge, MA: MIT Press, 1984, pp. 735-748.

[4] R. Dubey and J. Luh, "Redundant robot control for higher flexibility," in *Proc. IEEE Int. Conf. Robotics Automat.*, 1987, pp. 1066-1071.

[5] S. Lee, "Dual redundant arm configuration optimization with task-oriented dual arm manipulabilty," *IEEE Trans. Robotics Automat.*, pp. 78-97, Feb. 1989.

[6] S. Chiu, "Control of redundant manipulators for task compatibility," in *Proc. IEEE Int. Conf. Robotics Automat.*, 1987, pp. 1718-1724.

[7] ——, "Task compatibility of manipulator postures," *Int. J. Robotics Res.*, vol. 7, no. 5, pp. 13-21, Oct. 1988.

[8] J. Baillieul, "Kinematic programming alternatives for redundant manipulators," in *Proc. Int. Conf. Robotics Automat.*, 1985.

[9] L. Kelmar and P. Khosla, "Automatic generation of kinematics for a reconfigurable modular manipulator system," in *Proc. IEEE Int. Conf. Robotics Automat.*, 1988, pp. 663-668.

[10] S. Geman and D. Geman, "Stochastic relaxation, Gibbs distribution, and the Bayesian restoration of images," *IEEE Trans. Pattern Anal. Machine Intell.*, vol. 6, pp. 721-741, Nov. 1984.

[11] M. Vecchi and S. Kirkpatrick, "Global wiring by simulated annealing," *IEEE Trans. Computer-Aided Design*, pp. 215-222, Oct. 1983.

[12] S. Kirkpatrick, G. Gelett, and M. Vecchi, "Optimization by simulated annealing," *Science*, pp. 621-680, May 1983.

[13] N. Metropolis, A. Rosenbluth, M. Teller, and E. Teller, "Equations of state calculations by fast computing machines," *J. Chem. Phys.*, vol. 21, pp. 1087-1092, 1953.

[14] W. Carriker, P. Khosla, and B. Krogh, "An approach for coordinating mobility and manipulation," in *Proc. IEEE Int. Conf. Syst. Eng.*, Aug. 1989.

[15] R. Chatila and J. P. Laumond, "Position referencing and consistent world modelling for mobile robots," in *Proc. IEEE Int. Conf. Robotics Automat.*, 1985, pp. 138-145.

[16] R. Arkin, "Navigational path planning for a vision based mobile robot," *Robotica*, vol. 7, pp. 37-42, Jan. 1989.

[17] G. Miller and E. Wagner, "An optical rangefinder for autonomous robot," AT&T Bell Labs., Tech. Memo. TM 11228-870330-02, 1987.

[18] R. Horst and H. Tuy, "On the convergence of global methods in multiextremal optimization," *J. Opt. Theory Applications*, pp. 253-271, Aug. 1987.

[19] B. Hajek, "A tutorial survey of theory and applications of simulated annealing," in *Proc. 24th Conf. Decision and Control*, 1985, pp. 755-760.

[20] E. Aarts, J. Korst, and P. van Laarhoven, "A quantitative analysis of the simulated annealing algorithm: A case study of the traveling salesman problem," *J. Statistical Phys.*, vol. 50, no. 1/2, pp. 187-206, 1988.

[21] D. Mitra, F. Romeo, and A. Sangiovanni-Vancentelli, "Convergence and finite-time behavior of simulated annealing," in *Proc. IEEE Conf. Decision and Control*, 1985.

[22] D. Feng, M. Friedman, and B. Krogh, "The servo-control system for an omnidirectional mobile robot," in *Proc. IEEE Int. Conf. Robotics Automat.*, May 1989.


# Impedance Control with Adaptation for Robotic Manipulations

W.-S. Lu and Q.-H. Meng

*Abstract*—**Motivated by the algorithms of Craig *et al.* and of Slotine and Li for unconstrained motion control, two adaptive versions of impedance control are presented in this work. In our treatment, it has been assumed that some parameters in manipulator dynamics may be uncertain, and the measurements from the wrist force sensor utilized are imprecise. By introducing the concept of target-impedance reference trajectory (TIRT), which characterizes a desired dynamic relation of the end-point with the environment and a refined Lyapunov approach, it is shown that the adaptation mechanisms suggested by Craig *et al.* and Slotine and Li can be injected into Hogan's conventional impedance control. The two resulting algorithms are compared in terms of implementation feasibility as well as computation efficiency. Simulation results are presented to illustrate the proposed algorithms.**

## I. Introduction

Stable execution of contact tasks by mechanical manipulators has been identified as one of the major challenges in robotics [1]-[3], and a great deal of researchers' attention has been attracted to the problem during the past decade. Among several proposed control schemes, it appears that the impedance control of Hogan [4], [5] provides an unified approach to unconstrained motion control, obstacle avoidance, and constrained manipulation. In addition, it has

Manuscript received January 11, 1990; revised October 3, 1990. This work was supported by the Government of Canada under the Networks of Excellence Program. Portions of this paper were presented at the Third International Symposium on Robotics and Manufacturing, Vancouver, BC, Canada, July 1990.

The authors are with the Department of Electrical and Computer Engineering, University of Victoria, Victoria, BC, V8W 3P6, Canada.

IEEE Log Number 9144463.

theoretically been shown that the approach may also preserve motion stability during the contact between the end-effector and the environment [3]. This is a property especially attractive to the field of contact-force control [1].

As in the computed-torque servo for unconstrained motion control [6], [7], implementation of impedance control requires the use of accurate manipulator dynamics in its operational space as well as perfect measurements of the external force [5, eq. (23)]. On the other hand, some parameters in the manipulator's model such as moments of inertia or position of the center of mass in the end-effector may be uncertain due, e.g., to unpredictable payload changes [8]. In addition, measurements from a wrist force sensor are often found noisy. Model uncertainties of this type and imperfection of the force measurements could severely degrade the performance of a model/sensor-based robot controller such as impedance control [5, pp. 1051-1052] and, therefore, feasible compensation methods must be sought so as to maintain performance quality as well as motion stability in the presence of parameter uncertainties and measurement noise.

Motivated by the algorithm of Craig *et al.* [9] and of Slotine and Li [8] for unconstrained motion control, two adaptive versions of impedance control are presented in this work. As mentioned in [9], the method proposed there "might also be extended to include an active force control servo," but such an extension has not been as yet available to date. Slotine and Li [10] extended the method of [8] to include constrained manipulations but only the hybrid control [11] was considered. In addition, adaptive impedance control was identified as one of the aspects of adaptive control of constrained tasks that are worthy of further investigation, as stated in the concluding remarks of [10].

The difference of an adaptive impedance control from an adaptive unconstrained motion control is twofold. First, unlike unconstrained motion control, effort must be made to prevent performance degradation due to imperfection of the force sensor used. Second, here one deals with the dynamic interaction between the robot end-point and its environment that could be very rigid in many applications, and, as a reflection of this fact, regulation error must be redefined in order to accommodate the interactions that do not exist in the free-motion case. By introducing the concept of target-impedance reference trajectory (TIRT), which characterizes the desired dynamic relations of the end-point with the environment, it will be shown that the adaptation mechanisms of Craig *et al.* and Slotine and Li can be injected into Hogan's conventional impedance control. It will also be shown that the Lyapunov approach utilized in [8] and [9] can be refined to properly compensate the measurement noise as long as the magnitude of the noise is assumed to have a known bound.

This short paper is organized as follows. In Section II, the manipulator dynamics to be used throughout the work is given, followed by two comments on the conventional impedance control that appear to be useful in understanding the algorithm. The main results are presented in Sections III and IV. Section III begins with a brief presentation of the impedance control with estimated dynamic parameters. The concept of TIRT is then introduced, based on which a parameter adaptation law similar to [9] is derived where properties of strict positive real (SPR) functions are employed. In addition, an extra control torque is introduced and determined through a Lyapunov-type analysis to suppress the measurement noise from the force sensor. In Section IV, the TIRT is again utilized to inject the adaptation mechanism of [8] into impedance control. The resulting control algorithm and parameter adaptation law are first described, followed by a comparison of the two proposed adaptive schemes in terms of implementation feasibility as well as computation efficiency. Simulation results of the proposed algorithms as applied to a two degree-of-freedom (d.o.f.) planar arm are described and compared in Section V. An appendix is attached to include a brief discussion on SPR functions.

## II. The Manipulator Model and Conventional Impedance Control

### A. The Manipulator Model

The dynamics of an $n$ d.o.f. manipulator can be described by

$$H(q)\ddot{q} + C(q, \dot{q})\dot{q} + g(q) + f(\dot{q}) = \tau - J^T F_{\text{ext}} \quad (1)$$

where $\tau$ is the $n \times 1$ vector of the joint torque supplied by the actuators; $q$ is the joint displacement vector, $H(q)$ is the $n \times n$ symmetric, positive definite mass matrix; $C(q, \dot{q})$, $g(q)$, and $f(\dot{q})$ represent torques due to centrifugal, gravity, and friction forces, respectively; $J$ is the $n \times 6$ configuration-dependent Jacobian that relates the joint velocity to the linear and angular velocities of the end-effector; and $F_{\text{ext}}$ denotes the force exerted by the end-effector on the environment and measured by a wrist force sensor.

When controlling the dynamic behavior of the end-effector/environment interaction comes to be a main concern, it is often desirable to describe the manipulator dynamics in its operational space. Assuming $n = 6$, the Cartesian space robot dynamics is given by [12]

$$H_x(x)\ddot{x} + C_x(x, \dot{x})\dot{x} + g_x(x) + f_x(\dot{x}) = J^{-T}\tau - F_{\text{ext}} \quad (2)$$

where $x$ is a six-dimensional vector representing the position and orientation of the manipulator gripper, and

$$H_x = J^{-T} H J^{-1}$$
$$C_x(x, \dot{x}) = J^{-T}\left(C - HJ^{-1}\dot{J}\right)J^{-1}$$
$$g_x = J^{-T} g$$
$$f_x(\dot{x}) = J^{-T} f.$$

### B. Two Remarks on the Conventional Impedance Control

In the impedance control, target impedance is usually specified by a higher level supervisory system as a second-order dynamics [5]

$$M(\ddot{x} - \ddot{x}_v) + B(\dot{x} - \dot{x}_v) + K(x - x_v) = -F_{\text{ext}} \quad (3)$$

where $x_v$ is the virtual trajectory that often coincides with the desired trajectory when no contact occurs. However, it would most likely correspond to positions beyond the robot's workspace during the contact in order to maintain a proper amount of contact force. We will return to this point when discussing simulation results of the proposed control strategy in Section V.

*Remarks*

1) Given manipulator dynamics (2) and target impedance (3), it is quite natural to use a constrained motion control counterpart of the well-known resolved acceleration algorithm [13] to assign a control torque $\tau$ such that the overall system dynamics coincides with that given in (3). Obviously, such a torque is given by $\tau = J^T F$ with

$$F = F_{\text{ext}} + C_x\dot{x} + g_x + f_x + H_x\{\ddot{x}_v - M^{-1}[B(\dot{x} - \dot{x}_v) + K(x - x_v) + F_{\text{ext}}]\} \quad (4)$$

i.e., in the notation of [5],

$$\tau = J^T\{W^{-1}[M^{-1}(K(x_v - L(\theta)) + B(\dot{x}_v - J\dot{\theta})) + \ddot{x}_v + JH^{-1}(C\dot{\theta} + g + f) - \dot{J}\dot{\theta}] + [I - W^{-1}M^{-1}]F_{\text{ext}}\} \quad (5)$$

where $L(\theta)$ represents the forward kinematics operator that maps a set of joint displacements into the corresponding end-point position/orientation, and $W = JH^{-1}J^T$ is the mobility tensor whose inverse is the actual inertia of the robot end-effector in operational space [4]. The control law (5) has been known as impedance control for constrained motion of robots where the major control task is to regulate the dynamic relation of the end-effector with the environment to be contacted. It follows from the above observation that impedance control is indeed a duality of the resolved acceleration control in the domain of constrained motion control.

2) Control law (5) can also be used for redundant manipulators where the Jacobian $J$ is full row-rank rectangular matrix over its workspace. Indeed, the introduction of mobility tensor $W$ in this case avoids performing an inverse operation for the rectangular Jacobian. On the other hand, the control torque given by (5) is not computationally efficient when the manipulator involved has six d.o.f. and its Jacobian is nonsingular over the workspace. As a matter of fact, it can readily be shown that the joint torque $\tau$ needed can be computed using the formula

$$\tau = H\ddot{\theta}^* + C\dot{\theta} + g + f + J^T F_{\text{ext}} \tag{6}$$

where $\ddot{\theta}^*$ is given by

$$\ddot{\theta}^* = (MJ)^{-1}\left[K(x_v - L(\theta)) + B(\dot{x}_v - J\dot{\theta}) + M\ddot{x}_v - \dot{J}\dot{\theta} - F_{\text{ext}}\right]. \tag{7}$$

One can therefore use the measurements from joint position/velocity sensors as well as wrist force sensor to compute $\ddot{\theta}^*$ and then adopt the recursive Newton–Euler (NE) computation scheme [14] to calculate the sum of the first four terms on the right-hand side of (6).

## III. Adaptive Impedance Control: Algorithm 1

In the adaptive impedance control algorithm proposed below, unknown model parameters are estimated at each control instant in a manner similar to that of [9]. This is made possible by redefining the regulation error as $x - x_t$ where $x_t$ reflects the desired target impedance.

### A. Impedance Control with Estimated Dynamics

Let $p$ and $\hat{p} \in R^{r\times 1}$ denote the vector of all unknown parameters in the robot dynamic equation (2) and its estimate from an adaptation law to be specified later [see (19)], respectively. The impedance control can be implemented if the estimated parameter values are used in (4) or (6). For the sake of simplicity, it is assumed that the Jacobian is a square and nonsingular matrix over the workspace. The control torque can then be written as

$$\tau = \hat{H}\ddot{\theta}^* + \hat{C}\dot{\theta} + \hat{g} + \hat{f} + J^T\hat{F}_{\text{ext}} + J^T F_c \tag{8}$$

where $\hat{H}$, $\hat{C}$, $\hat{g}$, and $\hat{f}$ are evaluated using estimated parameters, $\hat{F}_{\text{ext}}$ is the measurement of $F_{\text{ext}}$, and $F_c$ is a control force to be determined later [see (22)] to handle the measurement noise from the wrist force sensor

$$\ddot{\theta}^* = (MJ)^{-1}\left[K(x_v - L(\theta)) + B(\dot{x}_v - J\dot{\theta}) + M\ddot{x}_v - \dot{J}\dot{\theta} - \hat{F}_{\text{ext}}\right]. \tag{9}$$

Similar to the discussion in Section II-B, the recursive NE computation scheme [14] applies to (8) and (9), making it a numerically attractive formulation in implementing the proposed algorithm.

In order to perform an error analysis, however, it is more appropriate to write the control torque as $\tau = J^T F$ with

$$F = \hat{F}_{\text{ext}} + \hat{C}_x\dot{x} + \hat{g}_x + \hat{f}_x + \hat{H}_x\{\ddot{x}_v - M^{-1}[B(\dot{x} - \dot{x}_v) + K(x - x_v) + \hat{F}_{\text{ext}}]\} + F_c. \tag{10}$$

### B. The Target-Impedance Reference Trajectory

Given the desired end-point/environment relation (3), a target-impedance reference trajectory (TIRT) is a differentiable vector function $x_t(t)$ of time, which solves the second-order differential equation (3) with a proper set of initial conditions, e.g., $x_t(0) = x_v(0)$ and $\dot{x}_t(0) = \dot{x}_v(0)$, and with $F_{\text{ext}}$ replaced by $\hat{F}_{\text{ext}}$. Clearly, the TIRT as a function of time coincides with the desired tracking trajectory over the unconstrained motion duration simply because of $\hat{F}_{\text{ext}} = 0$. However, it may differ considerably from the preassigned virtual trajectory during the contact. This is particularly true when either the environment involved has a very high stiffness or the target impedance is assigned such that its dynamics has a pole sufficiently close to the $j\omega$ axis. To be specific, the TIRT $x_t(t)$ in the rest of the paper is defined as the unique solution of the initial-value problem

$$\begin{aligned} M\ddot{x}_t + B\dot{x}_t + Kx_t &= -\hat{F}_{\text{ext}} + (M\ddot{x}_v + B\dot{x}_v + Kx_v) \\ x_t(0) &= x_v(0) \\ \dot{x}_t(0) &= \dot{x}_v(0). \end{aligned} \tag{11}$$

An example will be given in Section V to show the difference between the TIRT and virtual trajectory of a robot arm.

A couple of remarks on the introduced concept are now in order. First, with measurements from the wrist force sensor and the given virtual trajectory, the TIRT can be found very quickly in each sampling duration by numerically integrating (11). Further notice that such numerical integration is necessary only during the contact since one may otherwise simply take $x_t(t) = x_v(t)$. Second, the importance of this concept is due to the fact that the essence of impedance control is to reform the dynamic relation for the end-point/environment interaction such that the end-point could move along the TIRT. The importance of (11) will become more apparent when an attempt is made to derive an error equation for end-effector's position in the next subsection.

### C. The Parameter Adaptation and Determination of $F_c$

Applying control law (10) to dynamic equation (2), simple algebra leads to

$$M(\ddot{x} - \ddot{x}_v) + B(\dot{x} - \dot{x}_v) + K(x - x_v) + \hat{F}_{ext} = M\hat{H}_x^{-1}\left[(\tilde{H}_x\ddot{x} + \tilde{C}_x\dot{x} + \tilde{g}_x + \tilde{f}_x) + F_c + \Delta F_e\right]$$

where $\tilde{H}_x = \hat{H}_x - H_x$, $\tilde{C}_x = \hat{C}_x - C_x$, $\tilde{g}_x = \hat{g}_x - g_x$, $\tilde{f}_x = \hat{f}_x - f_x$, and $\Delta F_e = \hat{F}_{\text{ext}} - F_{\text{ext}}$. As mentioned before, it is not the virtual trajectory but the TIRT that the end-point tries to follow. Consequently, the regulation error for the constrained motion is defined as $e = x - x_t$, and the error dynamics is obtained by combining the above equation with (11) as

$$\ddot{e} + B_n\dot{e} + K_n e = \hat{H}_x^{-1}(W_c\phi + F_c + \Delta F_e) \triangleq u \tag{12}$$

where $B_n = M^{-1}B$, $K_n = M^{-1}K$, and

$$W_c\phi = \tilde{H}_x\ddot{x} + \tilde{C}_x\dot{x} + \tilde{g}_x + \tilde{f}_x \tag{13}$$

with

$$\phi = \hat{p} - p$$

and $W_c$ a $6 \times r$ matrix depending on $\ddot{x}$, $\dot{x}$, $x$, and the known manipulator parameters. On comparing (12) with the error equation

(11) of [9], the following distinctions may be observed: 1) Equation (12) is established in the operational space rather than the joint space. 2) The left-hand side of (12) is a reflection of the desired target impedance rather than desired unconstrained motion. 3) A friction term has been included in (13) with the assumption that only viscous friction and dynamic Coulomb friction effects are modeled. 4) Sensor noise $\Delta F_e$ is present and the control force $F_c$ is included in the right-hand side to suppress $\Delta F_e$ using a Lyapunov approach as will now be demonstrated.

It follows from [9] and the Appendix that an augmented error vector may be formed as

$$e^* = \dot{e} + \Psi_c e \tag{14}$$

with $\Psi_c = \text{diag}(\psi_1, \ldots, \psi_n)$, $\psi_i \in (0, b_{n_i})$, and $b_{n_i}$ the $i$th diagonal element in $B_n$ so that the input/output map $u \mapsto e^*$ admits a state-space description given by

$$\begin{aligned} \dot{X} &= \mathcal{A} X + \mathcal{B} u \\ e^* &= \mathcal{C} X \end{aligned} \tag{15}$$

where $X = [e_1 \ \dot{e}_1 \ \ldots \ e_n \ \dot{e}_n]^T$, $\mathcal{A} = \text{diag}(A_1, \ldots, A_n)$, $\mathcal{B} = \text{diag}(b_1, \ldots, b_n)$, and $\mathcal{C} = \text{diag}(c_1, \ldots, c_n)$ with

$$A_i = \begin{bmatrix} 0 & 1 \\ -k_{n_i} & -b_{n_i} \end{bmatrix}$$

$$b_i = \begin{bmatrix} 0 \\ 1 \end{bmatrix},$$

$$c_i = \begin{bmatrix} \psi_i & 1 \end{bmatrix}.$$

Note that transfer function matrix of system (15) is diagonal with all diagonal elements SPR. Consequently, there exist $\mathcal{P} = \text{diag}(P_1, \ldots, P_n) > 0$ and $\mathcal{Q} = \text{diag}(Q_1, \ldots, Q_n) > 0$ such that

$$\begin{aligned} \mathcal{A}^T \mathcal{P} + \mathcal{P} \mathcal{A} &= -\mathcal{Q} \\ \mathcal{P} \mathcal{B} &= \mathcal{C}^T. \end{aligned} \tag{16}$$

A Lyapunov-type error analysis begins by defining

$$V_c(X, \phi) = X^T \mathcal{P} X + \phi^T \Gamma_c^{-1} \phi \tag{17}$$

with $\Gamma_c$ positive definite. While the above Lyapunov function has been used in [9] for the unconstrained motion control problem, a careful treatment for the imprecise force measurements, which was not the issue in [9], is now needed. By (15)–(17)

$$\dot{V}_c = -X^T Q X + 2\phi^T \left( W_c^T \hat{H}_x^{-1} e^* + \Gamma_c^{-1} \dot{\hat{p}} \right) + 2 e^{*T} \hat{H}_x^{-1} (F_c + \Delta F_e). \tag{18}$$

Thus, the parameter adaptation law

$$\dot{\hat{p}} = -\Gamma_c W_c^T \hat{H}_x^{-1} e^* \tag{19}$$

leads (18) to

$$\dot{V}_c = -X^T Q X + 2 e^{*T} \hat{H}_x^{-1} (F_c + \Delta F_e). \tag{20}$$

If the measurement noise $\Delta F$ has a known bound, i.e.,

$$\| \Delta F_e \| \le \delta \tag{21}$$

then by choosing

$$F_c = -\frac{\gamma}{2} \hat{H}_x e^* \tag{22}$$

where $\gamma \ge 0$ is the gain factor to be determined later, we obtain

$$\dot{V}_c \le -\alpha - \gamma \beta^2 + 2\mu\delta \tag{23}$$

where

$$\begin{aligned} \alpha &= X^T Q X \\ \beta &= \| e^* \| \end{aligned}$$

and

$$\mu = \| \hat{H}_x^{-1} e^* \|.$$

Consequently, the time derivative of $V_c$ will be strictly negative if

(a) $X \neq 0$ and $e^* = 0$

or

(b) $X \neq 0$, $e^* \neq 0$, and

$$\alpha > 2\mu\delta$$

or

(c) $X \neq 0$, $e^* \neq 0$, $\alpha \le 2\mu\delta$, and

$$\gamma > \frac{2\mu\delta - \alpha}{\beta^2}. \tag{24}$$

If condition (a) or (b) is satisfied, (20)–(23) indicate that $F_c$ is not needed, i.e., one may assume $F_c = 0$. Otherwise, the term $F_c$ given by (22) with $\gamma$ satisfying (24) must be included in the control torque specified by (8) to guarantee a negative $\dot{V}_c$. In other words, the term $F_c$ in (8) can be specified by (22) with $\gamma$ satisfying

$$\gamma > \max\left(0, (2\mu\delta - \alpha)/\beta^2\right). \tag{25}$$

Furthermore, since in case (c) $\mu$ satisfies $\mu \ge \alpha/2\delta$ and $\mu \le \| \hat{H}_x^{-1} \| \beta$, we have $\beta \ge \alpha/(2\delta \| \hat{H}_x^{-1} \|)$ which implies that the right-hand side of (24) has an upper bound

$$\frac{2\mu\delta - \alpha}{\beta^2} \le \frac{4\delta^2 \| \hat{H}_x^{-1} \|^2 \left(2\beta\delta \| \hat{H}_x^{-1} \| - \alpha\right)}{\alpha^2} \equiv \gamma^*. \tag{26}$$

Obviously, $\gamma^*$ defined in (26) gives an indication of how large the gain factor $\gamma$ satisfying (24) [and hence (25)] might be for a given noise bound $\delta$.

In summary, (8), (14), (19), (22), and (25) have provided an adaptive version of Hogan's impedance control for a robot manipulator with uncertain parameters and an imperfect force sensor.

*Remarks*

1) In (2), (8), and (10), etc., it has been implicitly assumed that no singularities will occur along the planned motion trajectory. Effective approaches to avoiding singular configurations can be found in the literature; see, e.g., [17, ch. 7] and the references therein.

2) As in the unconstrained motion case [9], it follows from (13) and (19) that implementation of the proposed algorithm requires the invertibility of $\hat{H}_x$ and the use of joint acceleration. Moreover, (19) does not guarantee *a priori* that $\hat{H}_x^{-1}$ remains bounded [18]. A remedy for this difficulty is to replace (19) by a modified adaptive law suggested in [18, Sec. III-C] in which only a single $\hat{H}_x^{-1}$ with *fixed* parameters is needed.

### D. A Robustness Property of the Algorithm

There are a number of cases in which some or all components of the control torque $\tau$ calculated from (8) exceed the maximum torques that the actuators can provide, and, consequently, saturation occurs. In what follows we consider one such case where saturation is due to an unusually large force measurement $\hat{F}_{\text{ext}}$. Assume that $\hat{H}_x^{-1}$ is uniformly bounded, i.e.

$$\| \hat{H}_x^{-1} \| \le h^* \tag{27}$$

for some constant $h^* > 0$, and that the measurement noise from the force sensor is controlled by a known bound $\delta$ as in (21). Denoting by $\tau_{\text{sat}}$, the saturated controller output and $F_{\text{sat}} = J^{-T} \tau_{\text{sat}}$, the end-point force during the saturation can be written as

$$F_{\text{sat}} = F + \Delta F_s$$

where $\Delta F_s$ is defined as

$$\Delta F_s = F_{\text{sat}} - F$$

with $F$ obtained from (10). Obviously, with this $F_{\text{sat}}$ as the control force, the error dynamics equation (12) should be modified as

$$\ddot{e} + B_n\dot{e} + K_n e = \hat{H}_x^{-1}(W_c\phi + F_c + \Delta F_e + \Delta F_s) \triangleq u_s$$

which leads to the following modification of (23)

$$\dot{V}_c \le -\alpha - \gamma\beta^2 + 2\mu(\delta + \|\Delta F_s\|).$$

By (27) we have

$$\dot{V}_c \le -\alpha - \gamma\beta^2 + 2h^*(\delta + \|\Delta F_s\|)\beta. \tag{28}$$

It follows that the saturation may lead to a positive $\dot{V}_c$ and hence an increasing error signal $X$ (which is equivalent to $e$ and $\dot{e}$). On the other hand, since both $\alpha$ and $\beta^2$ are proportional to *square* of $\|e\| + \|\dot{e}\|$, (28) indicates that $\dot{V}_c$ will become negative again before the error gets too large. In other words, as may be expected, saturation of this type certainly causes a relatively large error as compared to that in an unsaturated control, but robust stability of the error dynamics is preserved for tasks in which the contact force may occasionally go up to a level causing controller saturation.

## IV. Adaptive Impedance Control: Algorithm 2

### A. The Control Algorithm and Parameter Adaptation

Again the TIRT is employed to form the regulation error

$$e = x - x_t. \tag{29}$$

The augmented error vector is defined as

$$s = \dot{e} + \Psi_s e \tag{30}$$

where $\Psi_s > 0$, but other constraints that were imposed on $\Psi_c$, its counterpart in algorithm 1 [see (14)], are now not needed. Further, let $x_r(t)$ be such that

$$\dot{x}_r = \dot{x} - s. \tag{31}$$

The second proposed adaptive impedance control is then given by

$$F = \hat{H}_x\ddot{x}_r + \hat{C}_x\dot{x}_r + \hat{g}_x + \hat{f}_x + \hat{F}_{\text{ext}} - K_d s \tag{32}$$

where $K_d > 0$, and $\hat{H}_x$, $\hat{C}_x$, $\hat{g}_x$, and $\hat{f}_x$ are obtained by substituting the estimated parameters $\hat{p}$ into $H_x, C_x, g_x, f_x$, respectively.

Defining

$$V_s(s,\phi) = \frac{1}{2}\left(s^T H_x s + \phi^T\Gamma_s^{-1}\phi\right)$$

which is an operational space counterpart of the Lyapunov function utilized in [10], (2), (31), (32), and the fact that $\dot{H}_x - 2C_x$ is skew-symmetric lead to

$$\dot{V}_s = \phi^T\left(W_s^T s + \Gamma_s^{-1}\dot{\phi}\right) - s^T K_d s + s^T\Delta F_e.$$

Consequently, if the adaptive law

$$\dot{\hat{p}} = -\Gamma_s W_s^T s \tag{33}$$

is used where $W_s$ is determined by

$$W_s\phi = \tilde{H}_x\ddot{x}_r + \tilde{C}_x\dot{x}_r + \tilde{g}_x + \tilde{f}_x \tag{34}$$

then

$$\dot{V}_s = -s^T K_d s + s^T\Delta F_e \le -\underline{k}_d\|s\|^2 + \delta\|s\| \tag{35}$$

where $\underline{k}_d$ denotes the smallest eigenvalue of $K_d$ and (21) has been assumed. Unlike the unconstraint motion case [10], (35) indicates that an *arbitrarily* chosen $K_d > 0$ could yield a positive $\dot{V}_s$ when $\|s\|$ is sufficiently small, $\|\Delta F_e\|$ is large, and the inner product $s^T\Delta F_e$ is positive. Nevertheless, the following analysis shows that the error signal $s$ (hence $e$ and $\dot{e}$) due to the sensor noise is bounded, and the bound can be reduced if more powerful actuators are available.

The boundedness of $\|s\|$ is an immediate consequence of (35): For a fixed $\underline{k}_d$, $\dot{V}_s < 0$ whenever $\|s\| > \delta/\underline{k}_d$, and a negative $\dot{V}_s$ means a reducing $V_s$ (versus time $t$) and hence $s$. The above argument also indicates that a larger $\underline{k}_d$ implies a smaller bound for $\|s\|$. By (32), it is observed that a large $\underline{k}_d$ (therefore a "large" $K_d$) may saturate the controller unless the actuators used are sufficiently powerful. Furthermore, (30) can be written in an integral form as

$$e(t) = e^{-\Psi_s(t-t_0)}e(t_0) + \int_{t_0}^{t} e^{-\Psi_s(t-\nu)}s(\nu)\,d\nu$$

which implies that

$$\|e(t)\| \le \|e^{-\Psi_s(t-t_0)}e(t_0)\| + \|s\|\int_{t_0}^{t}\|e^{-\Psi_s(t-\nu)}\|\,d\nu$$

$$\le \|e(t_0)\| + \|s\|/\underline{\psi}_s$$

where $\underline{\psi}_s$ is the smallest eigenvalue of $\Psi_s$. Therefore, the boundedness of $\|s\|$ implies the boundedness of $\|e\|$. Finally, (30) gives

$$\|\dot{e}\| \le \|s\| + \|\Psi_s\|\,\|e\|$$

i.e., the boundedness of $\|\dot{e}\|$.

In summary, (29)–(33) provide a natural combination of Hogan's impedance control with the Slotine–Li parameter adaptation. As is seen from the above argument, the robust stability of the error dynamics has been preserved, and the error $s$ (as well as $e$ and $\dot{e}$) may be further reduced by increasing gain $K_d$ as long as the actuators are sufficiently powerful. Finally, a Lyapunov-type analysis similar to that used in Section III-D may be applied to conclude that when the controller is saturated due to a large external force/torque, or a sensor failure, the control error will likely increase but remain bounded.

### B. Comparison of the Two Algorithms

As implementation feasibility of the algorithms is concerned, note that by (29)–(31)

$$\ddot{x}_r = \ddot{x}_t - \Psi_s\dot{e}.$$

Namely, algorithm 2 does not require the acceleration of end-effector $\ddot{x}$ for computing $F$ in (32) and $W_s$ in (34). Moreover, algorithm 2 does not need the inversion of $\hat{H}_x$ in updating parameter vector $\hat{p}$ as is seen from (33). On the contrary, $\ddot{x}$ and $\hat{H}_x^{-1}$ are required in implementing algorithm 1 as was mentioned in remark 2 in Section III-C. For those cases where the parameters to be identified are time invariant or slowly time varying, however, the rate for updating $\hat{p}$ may be chosen much lower than the control rate so that the implementation complexity of algorithm 2 due to the evaluation of $\ddot{x}$ and $\hat{H}_x^{-1}$ may be substantially reduced.

To compare computation efficiency of the algorithms, we first note that unlike algorithm 1, the recursive NE computation scheme does not directly apply to (32) of algorithm 2. By (31), it is, however, possible to reform (32) as

$$F = \hat{H}_x\ddot{x}_r + \hat{C}_x\dot{x} + \hat{g}_x + \hat{f}_x + \hat{C}_x s + \hat{F}_{\text{ext}} - K_d s$$

where sum of the first four terms can be calculated using NE recursion, and the fifth term $\hat{C}_x s$ may be ignored when $s$ is small and the robot motion is slow (which is very likely the case in a contact task). Another approach to reducing the computation burden of algorithm 2 is to express control torque $F$ as

$$F = W_s\hat{p} + \hat{F}_{ext} - K_d s \tag{36}$$

where $W_s$ has been determined by (34).

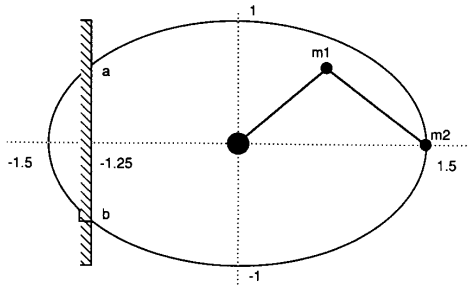


Fig. 1. The robot manipulator and assigned virtual trajectory.

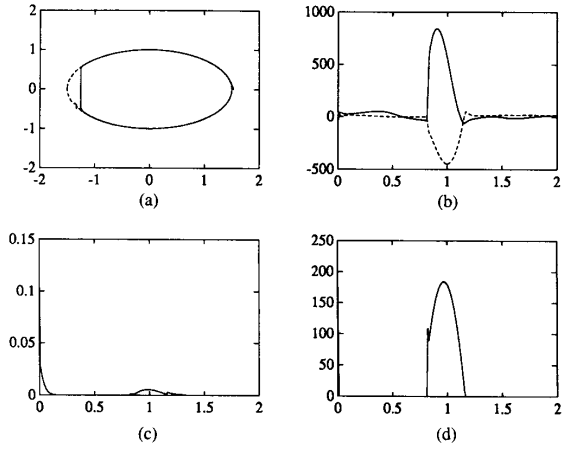


Fig. 2. Conventional impedance control with true value of $m_2$ ($m_2 = 1$ kg). (a) Ideal and actual trajectories. (b) Control torques. (c) Tracking error in meters. (d) Contact force.

## V. Simulation Results

A 2 d.o.f. planar robot was used in the simulation to verify the proposed algorithms. As shown in Fig. 1, the robot motion begins at point (1.5, 0) moving along an elliptic trajectory until the end-point of the robot hits a wall at point $a$. The end-point is then required to be in proper contact with the wall while sliding down to point $b$ along the surface of the wall. The end-point then leaves the wall moving back to point (1.5, 0) along the elliptic trajectory. It is assumed that the mass of each link is a point mass located at the distal end of the link. The true mass values are $m_1 = 2$ kg, $m_2 = 1$ kg, where $m_2$ represents 0.5-kg link mass plus a 0.5-kg payload, and the link lengths are $l_1 = l_2 = 1m$. The major portion of the virtual trajectory $x_v(t) = [x_{1v}(t)\ x_{2v}(t)]^T$ is an ellipse described by

$$x_{1v}(t) = 1.5\cos \pi t$$
$$x_{2v}(t) = \sin \pi t$$

for $0 \le t \le 2$ s, but as is shown in Fig. 1, there is a small straight segment replacing the elliptic arc in order to maintain proper contact force.

Assuming that all parameters of the robot manipulator are precisely known and a perfect force sensor is used, Fig. 2 shows the simulation results when the conventional impedance control (5) is employed, where the parameters in target impedance characterization (3) are chosen as $B = 2\sqrt{MK}$ with $M = 2$, $K = 4000$, and the environment is assumed to have a high stiffness $K_f = 10^5$. Fig. 3 shows the TIRT, i.e., $x_t(t)$ (dash line) and virtual trajectory (real line) of the robot. It is seen that $x_t(t)$ and $x_v(t)$ are nearly identical until a large external force applies to the gripper when it hits the wall. Next the simulation considers using the conventional impedance control algorithm (5) with parameter $m_2$ replaced by the incorrect value 2.5 kg. As is shown in Fig. 4, the robot motion then exhibits an unacceptable performance degradation.

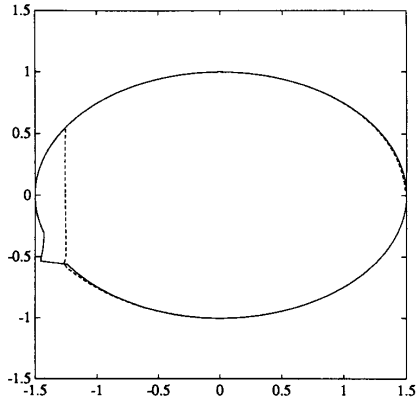

Fig. 3. The TIRT versus virtual trajectory of the robot.

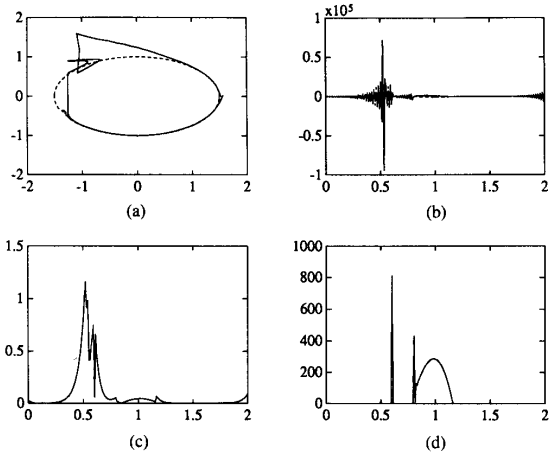


Fig. 4. Conventional impedance control with $m_2 = 2.5$ kg. (a) Ideal and actual trajectories. (b) Control torques. (c) Tracking error in meters. (d) Contact force.

The target impedance in the adaptive control case is set as $B = 340$, $M = 2$, and $K = 4000$. For the comparison purpose, $m_2$ is treated as the only unknown parameter in the manipulator's model and an initial guess of $m_2 = 2.5$ kg is made for the two proposed algorithms. In addition, $\hat{F}_{ext}$ in the simulation is assumed to be $F_{ext}$ plus a normally distributed random noise whose maximum magnitude is about 15% of the peak value of the contact force. By applying Algorithm 1 and assuming no controller saturation, the actual (real line) and the pre-assigned virtual trajectory (dash line), the estimated values of $m_2$, the tracking error, and the contact force are shown in Fig. 5. Next it is assumed that the actuators can only provide 75% of the maximum torque required in the preceding simulation. As shown in Fig. 6, in such a case the same algorithm leads to larger tracking errors and larger contact force errors, but the overall performance remains acceptable. Finally, algorithm 2 is applied and the results are shown in Fig. 7. It is found that the

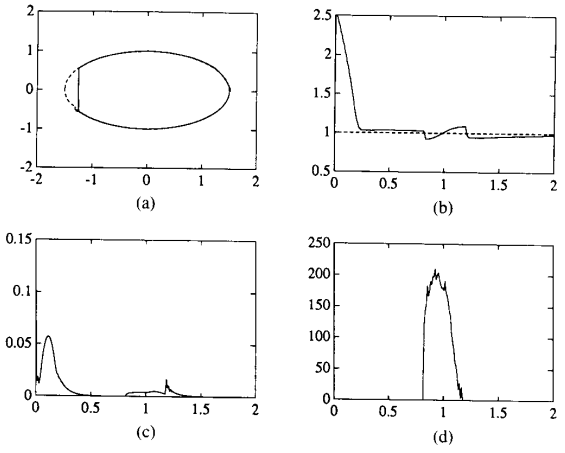


Fig. 5. Adaptive impedance control using algorithm 1 without saturation. (a) Ideal and actual trajectories. (b) Estimated $m_2$. (c) Tracking error in meters. (d) Contact force.

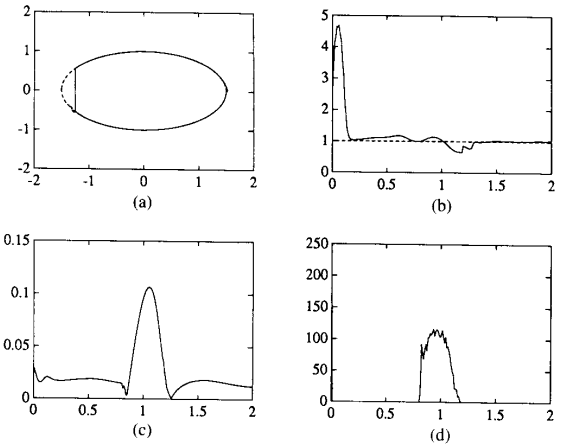


Fig. 6. Adaptive impedance control using algorithm 1 with saturation. (a) Ideal and actual trajectories. (b) Estimated $m_2$. (c) Tracking error in meters. (d) Contact force.

control torques required by algorithm 2 to perform the same task is considerably less than that needed in algorithm 1. Consequently, the controller will not be saturated even if only 75% of the maximum torques required by algorithm 1 is available. It is noted that the tracking errors remain very small during the free-motion period, but both tracking errors and contact force errors are slightly larger than that achieved by algorithm 1 in the nonsaturation case. Also note that the estimated value of $m_2$ in all cases quickly approaches to its true value 1 kg during the first free-motion duration. It is then followed by some fluctuation with a less than 20% maximum deviation during the contact and a recovery as soon as the end-effector leaves from the wall at point $b$.

As discussed in Section IV, algorithm 2 proposed there appears to be computationally more efficient as compared with algorithm 1. In addition, from a number of computer simulations carried out so far, it is found that parameters $\Psi_s$ and $\Gamma_s$ in algorithm 2 are less sensitive than their counterparts $\Psi_c$ and $\Gamma_c$ in algorithm 1 in order to complete a stable execution of a contact task.

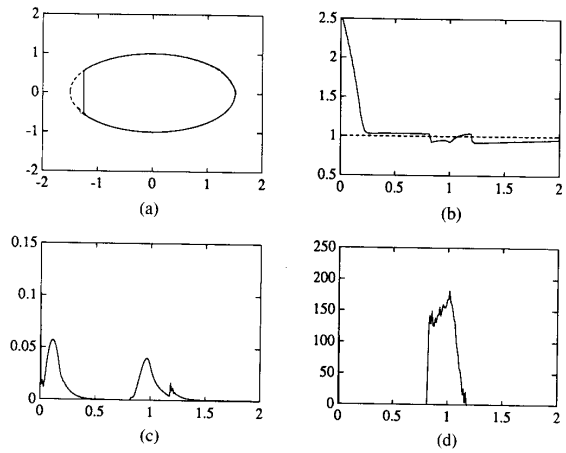


Fig. 7. Adaptive impedance control using algorithm 2. (a) Ideal and actual trajectories. (b) Estimated $m_2$. (c) Tracking error in meters. (d) Contact force.

## VI. Conclusions

The adaptive laws of Craig *et al.* and of Slotine and Li have been extended to establish two adaptive versions of Hogan's impedance control for stable execution of contact tasks. In our development, the wrist force sensor has been assumed to be imperfect. The extensions are made possible by introducing the concept of TIRT in conjunction with the refined Lyapunov approach, which are similar to those employed in [9] and [8].

Simulation results reported in this paper indicate that severe performance degradation due to parameter uncertainties in an impedance-controlled robotic system can be prevented by utilizing one of the two adaptive impedance control algorithms proposed in this paper.

## Appendix
## Strictly Positive Real Functions

The concept of strictly positive real functions (SPR) has been extensively studied for more than two decades [15], [16] and has found numerous applications in network analysis, robustness analysis, nonlinear control, and adaptive control. A proper rational function $f(s)$ is said to be SPR if the real part of $f(j\omega)$ is strictly greater than zero for all $\omega \in R$. As an example, consider second-order stable transfer function

$$f(s) = \frac{s + \psi}{s^2 + k_v s + k_p} \tag{A1}$$

where $k_v > 0$, $k_p > 0$ are given, and $\psi$ is a system parameter. It is easy to verify that $f(s)$ is SPR if $0 < \psi < k_v$. When a stable SPR rational function is realized in a state space, the passive nature of such a transfer function provides a system-theoretic property that is more valuable than a single Lyapunov equation does. Indeed, if function $f(s)$ given by (A1) with $\psi \in (0, k_v)$ is realized as $\Sigma = (A, b, c)$ where

$$A = \begin{bmatrix} 0 & 1 \\ -k_p & -k_v \end{bmatrix}$$

$$b = \begin{bmatrix} 0 \\ 1 \end{bmatrix}$$

and

$$c = [\psi \quad 1]$$

it can then be shown that there exist two positive definite matrices $P$ and $Q$ such that

$$A^T P + PA = -Q$$
$$Pb = c^T. \tag{A2}$$

The combination of the two equations in (A2) plays a crucial role in deriving an adaptive control law for unconstrained motion control [9]. Notice that one solution to (A2) is given by

$$P = \begin{bmatrix} k_p + \psi k_v & \psi \\ \psi & 1 \end{bmatrix}$$
$$Q = \begin{bmatrix} 2\psi k_p & 0 \\ 0 & 2(k_v - \psi) \end{bmatrix}$$

both of which are positive definite with $\psi \in (0, k_v)$. A thorough discussion on time domain and frequent domain conditions for strict positive realness can be found in [16].

## Acknowledgment

The authors are members of the Institute for Robotics and Intelligent Systems (IRIS) and wish to acknowledge the support of the Networks of Excellence Program of the Government of Canada and the participation of PRECARN Associates Inc.

## References

[1] D. E. Whitney, "Historical perspective and state of the art in robot force control," in *Proc. IEEE. Conf. Robotics Automat.*, 1985, pp. 262-268.

[2] R. P. Paul, "Problems and research issues associated with the hybrid control of force and displacement," in *Proc. IEEE Conf. Robotics Automat.*, 1987, pp. 1966-1971.

[3] N. Hogan, "On the stability of manipulators performing contact tasks," *IEEE J. Robotics Automat.*, vol. 4, pp. 667-686, 1988.

[4] ___, "Impedance control: An approach to manipulation: Part I—Theory, Part II—Implementation, Part III—Applications," *ASME J. Dyn. Syst., Meas., Control*, vol. 107, pp. 1-24, 1985.

[5] ___, "Stable execution of contact tasks using impedance control," in *Proc. IEEE Conf. Robotics Automat.*, 1987, pp. 1047-1054.

[6] R. P. Paul, "Modeling, trajectory calculation, and servoing of a computer controlled arm," Stanford Artificial Intelligence Lab., Stanford Univ., Memo AIM-177, 1972.

[7] A. K. Bejczy, "Robot arm dynamics and control," JPL, California Institute of Technology, TM 33-69, 1974.

[8] J.-J. E. Slotine and W. Li, "Adaptive manipulator control: A case study," in *Proc. IEEE Int. Conf. Robotics Automat.* 1987, pp. 1392-1400.

[9] J. J. Craig, P. Hsu, and S. S. Sastry, "Adaptive control of mechanical manipulators," in *Proc. IEEE Conf. Robotics Automat.*, 1986, pp. 190-195.

[10] J.-J. E. Slotine and W. Li, "Adaptive strategies in constrained manipulation," in *Proc. IEEE Int. Conf. Robotics Automat.*, 1987, pp. 595-601.

[11] M. H. Raibert and J. J. Craig, "Hybrid position/force control of manipulators," *ASME J. Dyn. Syst., Meas., Control*, vol. 102, pp. 126-133, June 1981.

[12] J. J. Craig, *Introduction to Robotics*, 2nd ed. Reading MA: Addison-Wesley, 1989.

[13] J. Y. S. Luh, M. W. Walker, and R. P. Paul, "Resolved acceleration control of mechanical manipulators," *IEEE Trans. Automat. Control*, vol. AC-25, pp. 468-574, 1980.

[14] ___, "On-line computational scheme for mechanical manipulators," *ASME J. Dyn. Syst., Meas., Control*, vol. 102, pp. 69-76, 1980.

[15] B. D. O. Anderson and S. Vongpanitlerd, *Network Analysis and Synthesis—A Modern System Theory Approach*. Englewood Cliffs, NJ: Prentice-Hall, 1973.

[16] J. T. Wen, "Time domain and frequency domain conditions for strict positive realness," *IEEE Trans. Automat. Control*, vol. 33, pp. 988-992, 1988.

[17] T. Yoshikawa, *Foundations of Robotics: Analysis and Control*. Cambridge, MA: MIT Press, 1990.

[18] M. W. Spong and R. Ortega, "On adaptive inverse dynamics control of rigid robots," *IEEE Trans. Automat. Control*, vol. 35, pp.92-95, Jan. 1990.